

Numerical Methods Final Project

Bashar Karaja

February 5, 2024

1 Introduction

In this report, we explore applying the localized Green's function method to solve the one-dimensional time-independent Schrödinger equation, particularly in configurations relevant to modeling electron scattering by quantum junctions. We examine potential profiles featuring variable barriers by focusing on resonant tunneling devices in GaAs-AlGaAs heterostructures. Our investigation aims to analyze reflection, transmission, and absorption coefficients, considering the effect of bias and exploring energy bounds. Through this study, we aim to deepen our understanding of quantum transport phenomena, essential for advancing quantum electronic devices.

NOTE: all the coding files written respect the MATLAB format and might not be totally compatible with OCTAVE. Kindly run the coding files on MATLAB and not OCTAVE to ensure no errors occur.

2 Methodology

In the initial stages of the computational process, the foundation is laid first by recognizing the green function of our system. In general, Green's function is a mathematical tool used to solve differential equations. In the context of quantum mechanics, Green's function method provides a systematic approach to solving the Schrödinger equation for complex systems.

Our project is mainly divided into two parts. The first part considers a reference system featuring a constant potential background $U_0 = 0$ for all spatial positions x , where the green's function for such case is defined as in eq.4.34 in the lecture notes:

$$G_0(x, x'; k) = \frac{e^{ik|x-x'|}}{2ik} \quad (1)$$

where The parameter k represents the wave vector associated with the particle or wave being described and x and x' are spatial positions where the green's function is evaluated.

The second part Consider a reference system featuring a step function $U_0(x \text{ less than } 0) = 0$ and $U_0(x \text{ greater than } 0) = U_1 = -0.1 \text{ eV}$ as potential background and therefore the green's function here is defined as in eq A.77 and A.76 in the lecture notes:

$$G_{+,+}(x, x'; z) = \frac{e^{ik_1|x-x'|}}{2ik_1} + \frac{k_1 - k_0}{k_1 + k_0} * \frac{e^{ik_1(x+x')}}{2ik_1} \quad (2)$$

for x larger than 0 and x' larger than 0. and,

$$G_{+,+}(x, x'; z) = \frac{e^{-ik_0x + ik_1x'}}{i(k_0 + k_1)} \quad (3)$$

for $-\infty < x < 0 < x'$

the electric field in the second part is defined as:

$$|E| = \frac{U_1}{x_{max} - x_{min}} \quad (4)$$

where $x_{max} - x'_{min}$ is the width of the heterostructure.

3 Analysis and Results

3.1 Constant background as reference system

Consider a reference system having a potential background $U_0 = 0 \forall x$.

we consider the potential profile of two barriers of the same height defined as :

$$U(x') = \begin{cases} 0.2\text{eV}; & \forall x' \in [0\text{\AA}, 15\text{\AA}] \\ 0.2\text{eV}; & \forall x' \in [65\text{\AA}, 80\text{\AA}] \\ 0 & \text{elsewhere} \end{cases} \quad (5)$$

Figure 1 shows the potential barriers plot.

since there is no potential barrier behind 0 eV, we can set the lower bound E_a to be 0. To prevent aliasing in our analysis, we must ensure that the energy step size adequately captures the variations in potential energy. We can follow a similar analogy to the Nyquist frequency in signal processing, where the sampling rate should be twice the

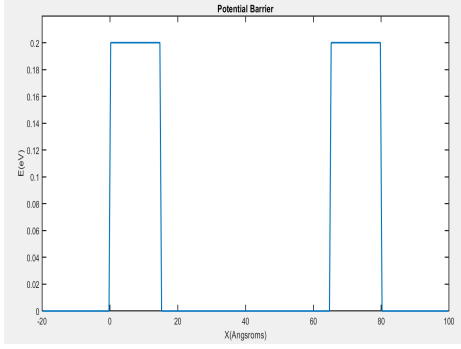


Figure 1: Potential Barrier, eq.7

highest frequency component to avoid distortion. Hence, we can set the upper bound E_b to be 0.4 eV. This approach guarantees that our discretization captures the energy dynamics effectively, akin to ensuring sufficient sampling.

3.1.1 Reflection, Transmission and absorption coefficients

we now consider an incident energy E_0 associated with an electron incident as a plane wave from $x=-\infty$, for E_0 [0eV, 0.3 eV] and using a 1 nanosecond recombination time (lifetime) parameter, the reflection, $R(E_0)$, transmission $T(E_0)$ and absorption coefficients $A(E_0)$ would be:

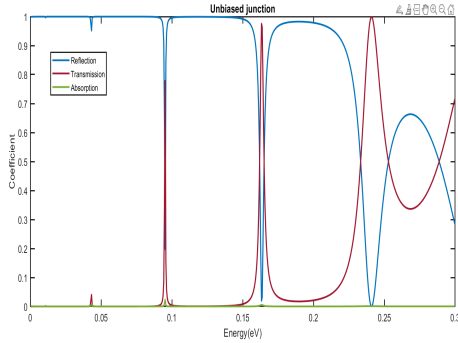


Figure 2: Reflection, Transmission and absorption coefficients graphs(R-T-A graph) before modification of the barriers,eq.7

In the Reflection, Transmission, and Absorption graph, a notable absence of transmission is evident before $E = 0.2$ eV, with the exception of multiple peaks indicating resonance, wherein the system efficiently transmits energy. These resonant peaks occur when the incoming wave's frequency aligns with the system's natural frequency, fostering constructive interference and heightened transmission efficiency. As the energy approaches and surpasses $E = 0.2$ eV, which is the value of the potential

barriers, the transmission gradually becomes observable and increases in magnitude.

Conversely, the reflection curve exhibits a contrasting trend, showcasing maximum reflection when no transmission is observed, and exhibiting dips coinciding with peaks in the transmission curve. As the energy escalates beyond $E = 0.2$ eV, reflection diminishes while transmission intensifies. Absorption remains minimal throughout the spectrum of energy variation, with only a very small peak observed near 0.1 eV.

In quantum mechanics, a resonance occurs when the incident energy matches a quasi-bound state within the scattering potential, leading to sharp peaks or dips in the transmission, reflection, or absorption coefficients. To determine resonance, we look for these peaks or dips in the coefficients as a function of energy.

3.1.2 Probability densities against barriers

From the R-T-A graph (figure 1) we can find multiple Resonance energies and non-resonant energy. The resonant energies taken are : [0.01075, 0.04325, 0.09525, 0.16325] and 0.07 eV for the non-resonant energy. the graphical representation of their respective probability densities against the barriers is shown in Figure 3 below:

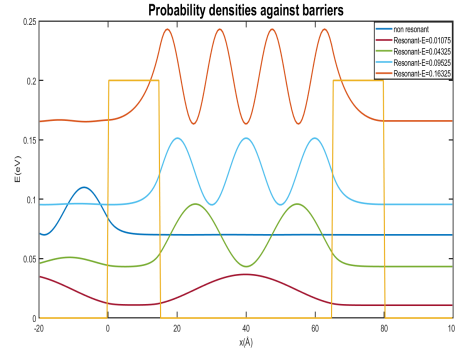


Figure 3: Probability densities against barriers

In Figure 3, we have analyzed four resonant energies discerned from the peaks observed in the transmission curve depicted in Figure 2, alongside a singular resonant frequency. The resonant curves exhibit distinct oscillatory patterns, each aligning with a resonant mode. Conversely, such oscillatory behavior was conspicuously absent in the non-resonant curve.

3.1.3 R-T-A Graph after potential profile modification

In this part, we now consider that the potential profile is modified to be as follows:

$$U(x') = \begin{cases} 0.2\text{eV}; & \forall x \in [0\text{\AA}, 15\text{\AA}] \\ 0.1\text{eV}; & \forall x \in [65\text{\AA}, 80\text{\AA}] \\ 0 & \text{elsewhere} \end{cases} \quad (6)$$

Therefore, the R-T-A graph is now different, which is shown in Figure 4:

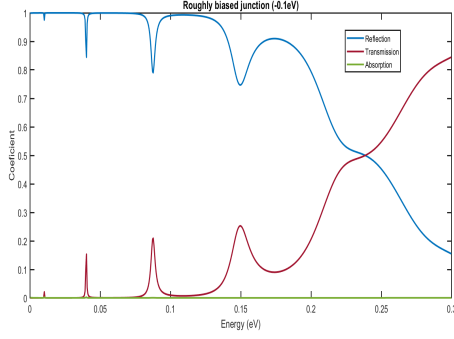


Figure 4: Reflection, Transmission and absorption coefficients after modification of the barriers, eq.8

Plotting both cases reveals that post-potential modification, the sharpness of reflection and transmission peaks diminishes compared to their pre-modification counterparts. In both scenarios, there's a noticeable decrease in the reflection coefficient and a corresponding increase in the transmission coefficient. However, an intriguing observation emerges: after the barrier modification, the transmission curve initiates its ascent at approximately 0.1 eV, coinciding with the new barrier value between 65 Angstroms and 80 Angstroms. This onset occurs earlier than what is observed in the pre-modification transmission curve, which exhibited an increase around 0.2 eV. Similarly, the reflection coefficient begins its descent concurrently with the transmission increase, around 0.1 eV—a shift also occurring earlier compared to the original case before barrier modification.

3.2 Step function as reference system

Consider a reference system featuring a step function U_0 defined as follows:

$$U_0(x) = \begin{cases} 0\text{eV}; & \forall x < 0 \\ U_1 = -0.1\text{eV}; & \forall x > 0 \end{cases} \quad (7)$$

For this reference system, the incident wave from $x = -\infty$ and the wave transmitted towards ∞ are then given by eq. (A.65) in the lecture notes:

$$y_b(x) = \begin{cases} e^{iK_0x} + r_b e^{-iK_0x} & \text{if } x < 0 \\ t_b e^{iK_1x} & \text{if } x > 0 \end{cases} \quad (8)$$

The electric field associated with this bias is thus given by:

$$|E| = -\frac{U_1}{x'_{\max} - x'_{\min}} \quad (9)$$

Then, the potential defined by eq.7 must be modified as follows:

$$W(x') = \begin{cases} U(x') - |E|x' & \text{if and only if } x'_{\min} < x' < x'_{\max} \end{cases} \quad (10)$$

the graph of the potential has now become:

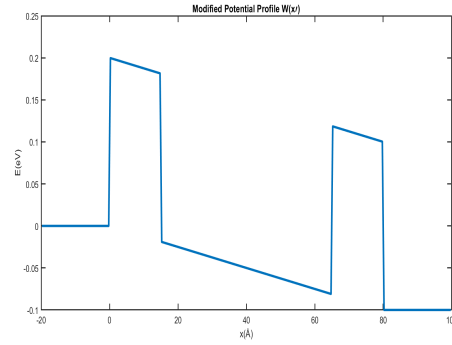


Figure 5: Modified potential $W(x')$

Similar to what we did in the previous section for the upper and lower bounds, we set $E_a = 0$ and $E_b = 0.8\text{eV}$

3.2.1 R-T-A graph

We will Follow a similar analogy as in section 3.1.1 of the report with the same recombination time of 1 nsec, except with the change of the potential to $W(x')$. The R-T-A graph thus becomes:

3.2.2 Effect of Bias

Here, we are modeling an electron at the Fermi level, where we now set $E_0 = 0.01\text{ eV}$ and explore the effect of tuning the bias, thereby meaning that U_1 belong to the interval $[0.2, 0.2]\text{ eV}$.

The graphs below figures 6 and 7, show the profile potentials for the two cases: U_1 is equal to 0.2 eV and U_1 is equal to 0.2 eV respectively:

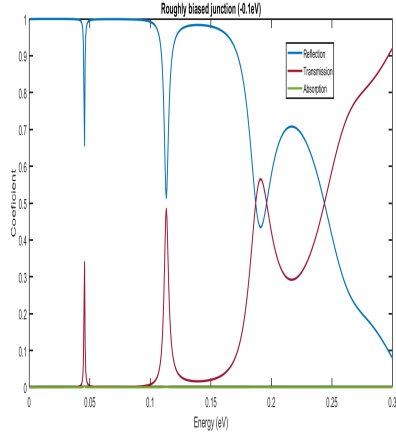


Figure 6: R-T-A graph considering the potential $W(x')$, eq.12

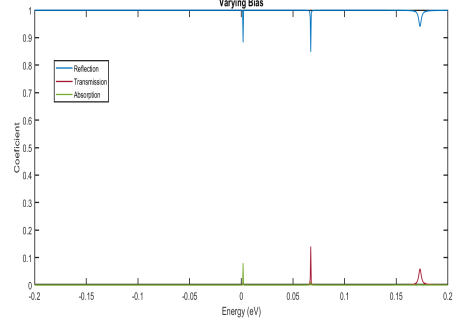


Figure 9: R-T-A graph as U_1 varies

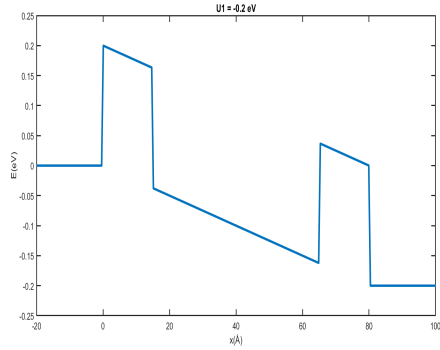


Figure 7: Potential profile for $U_1 = -0.2 \text{ eV}$

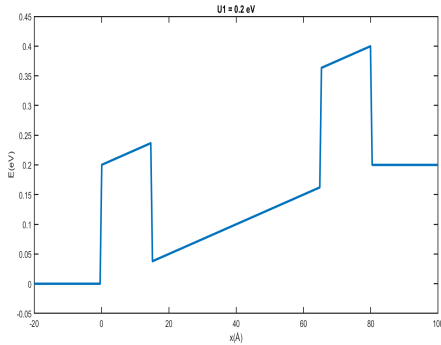


Figure 8: Potential profile for $U_1 = 0.2 \text{ eV}$

3.2.3 R-T-A Graph as U_1 Varies

Instead of varying the value of E_0 as in the previous cases, we now vary the value of U_1 by steps of 0.0005 eV such that $U_1 \in [-0.2, 0.2] \text{ eV}$. The R-T-A graph thus become as in Figure 9

In the scenario of varying potential, the spectrum exhibits a phenomenon known as Negative Differential Resistance (NDR). The potential profiles for junctions biased at -0.2 eV and 0.2 eV significantly influence electron flow and resonance. At -0.2 eV , the potential drop facilitates electron transition, potentially contributing to NDR by augmenting transmission up to the resonance point. Conversely, at 0.2 eV , the potential rise impedes electron flow, enhancing NDR as transmission sharply peaks at resonance and subsequently diminishes with increased misalignment of energy levels due to the bias.

The resulting current-voltage (I-V) curve, derived from the spectral characteristics of the junction under varying bias, is expected to exhibit non-linear behavior owing to the quantum mechanical effects in play. Transmission displays moderate peaks at biases approximately around 0.05 eV and 0.15 eV , with coefficients peaking at 0.1 and 0.05 , indicative of moderate increases in current at these energy levels due to resonant tunneling.

Outside these peaks, transmission remains low, accompanied by high reflection, indicating minimal current flow and resulting in flat regions on the I-V curve. These features deviate from the linear response of an ohmic resistor and also from the exponential I-V characteristic of a diode. Instead, the anticipated I-V curve is expected to display distinct moderate peaks at certain biases alongside flat regions, emphasizing the specialized behavior of the junction under the influence of quantum mechanics.

4 Conclusion

In our study of resonant tunneling devices in GaAs-AlGaAs heterostructures, we analyzed reflection, transmission, and absorption coefficients for incident energy E_0 ranging from 0 to 0.3 eV with a recombination time of 1 nanosecond. Below $E = 0.2$ eV, transmission was minimal except for resonant peaks indicating constructive interference. As energy surpassed $E = 0.2$ eV, transmission gradually increased, while reflection peaked. Post-potential modification, reflection and transmission peaks became less sharp. After modifying the barrier, the transmission ascent onset occurred earlier at around 0.1 eV compared to the original case. We identified multiple resonance and non-resonant energies and observed nonlinear behavior in the resulting current-voltage (I-V) curve, with moderate peaks indicating resonant tunneling effects. This behavior deviates from typical resistor or diode characteristics, emphasizing the specialized behavior of the junction under quantum mechanics' influence.

5 references

NUMERICAL-METHODS-FOR-
PHYSICISTS,Alain-Deraux-Lecture-Notes